Enhanced Quantum State Detection Efficiency through Quantum Information Processing

T. Schaetz,* M. D. Barrett,† D. Leibfried, J. Britton, J. Chiaverini, W. M. Itano, J. D. Jost, E. Knill, C. Langer, and D. J. Wineland

National Institute of Standards and Technology, 325 Broadway, Boulder, Colorado 80305, USA

(Received 4 March 2004; published 7 January 2005)

We investigate theoretically and experimentally how quantum state-detection efficiency is improved by the use of quantum information processing (QIP). Experimentally, we encode the state of one $^9Be^+$ ion qubit with one additional ancilla qubit. By measuring both qubits, we reduce the state-detection error in the presence of noise. The deviation from the theoretically allowed reduction is due to infidelities of the QIP operations. Applying this general scheme to more ancilla qubits suggests that error in the individual qubit measurements need not be a limit to scalable quantum computation.

DOI: 10.1103/PhysRevLett.94.010501 PACS numbers: 03.67.Lx, 03.67.Pp, 32.80.Qk, 42.50.Lc

A central feature of quantum information processing (QIP) is the use of conditional quantum logic to enhance the efficiency of performing certain algorithms or tasks [1]. One such task is the efficient quantum state measurement itself, which is one of the defining goals of metrology and an important component of QIP [2].

In the context of quantum computation, when the coherent operations used in an algorithm can be performed with higher efficiency than the state detection, or readout, the overall efficiency is restricted by the latter. This affects the abilities of quantum computation in three ways. First, it may require excessive repetition of an algorithm in order to reliably determine its output. Second, it can render a system unscalable because the required maximum tolerable error rate is not achieved for all operations including detection. Finally, even if scalability is in reach, the failure of measurements needed for error correction during the computation requires additional overhead to avoid miscorrecting errors. Fortunately, simple elements of QIP can be used to enhance state-detection efficiency.

Assume we are given a qubit, a two-state quantum system, where the wave function Ψ in a chosen measurement basis is specified by a superposition of two states $|0\rangle$ and $|1\rangle$, $|\Psi\rangle = \alpha_0|0\rangle + \alpha_1|1\rangle$. When a measurement operation is invoked, the qubit is projected into the eigenstate $|0\rangle$ ($|1\rangle$), with probability $|\alpha_0|^2$ ($|\alpha_1|^2$), where $|\alpha_0|^2 + |\alpha_1|^2 = 1$. For a series of measurements on identically prepared qubits in superposition states ($\alpha_0 \neq 0, 1$), the measurement outcomes fluctuate due to projection noise [3], a fundamental noise limit. However, due to the presence of additional technical noise in a real experiment, we sometimes determine that the qubit was in state $|0\rangle$ when it was actually in state $|1\rangle$, and vice versa. This can occur even if the qubit is in an eigenstate ($\alpha_0 = 0$ or 1) before the measurement operation and projection noise is absent. For a quantum algorithm such as Shor's factoring algorithm [4], the state of the system before the final measurement is a large superposition state of N qubits of the form $\beta_0|000\cdots0\rangle + \beta_1|000\cdots1\rangle + \cdots + \beta_{2^N-1}|111\cdots1\rangle$, where most β_k are 0, but there are still exponentially many nonzero β_k with similar magnitudes. When the measurement projection occurs, the information from the number k (not $|\beta_k|^2$) is then used in a classical algorithm to find a factor of the input number. Let the readout fidelity F be the probability of correctly measuring the state $|0\rangle$ or $|1\rangle$ for an individual qubit and assume equal probability of misidentifying these states. The fidelity of correctly obtaining all the bits of k in the readout process is given by F^N. For small F, the overall readout fidelity becomes exponentially small with N, or, conversely, we appear to require an exponentially large number of measurements and repetitions of the algorithm to determine a useful output k. The problem is avoided if $F \rightarrow 1$.

To improve state detection, a seemingly obvious strategy would be to run the algorithm many times to gain statistical precision. This is an undesirable solution for algorithms involving many coherent operations followed by a single measurement. Also if the algorithm requires a significant amount of error correction, detection errors compound and repetition may actually fail to give the desired result. Avoiding the repetition of the algorithm by copying the final state and measuring the copies is precluded by the impossibility of cloning superposition states [5]. However, a way to enhance state-detection fidelity by using quantum logic gates in conjunction with auxiliary ''ancilla'' qubits is outlined in Ref. [2]. For simplicity, consider a qubit in the superposition state $|\psi\rangle = \alpha_0|0\rangle + \alpha_1|1\rangle$. A sequence of M controlled-not gates [1] involving ancillae $\mathrm{a}1, \mathrm{a}2 \cdots \mathrm{a}M$ reserved for this qubit encodes $|\psi\rangle$ to an entangled state according to the transformation

$$(\alpha_0|0\rangle + \alpha_1|1\rangle)|0\rangle_{\mathrm{a}1}|0\rangle_{\mathrm{a}2}\cdots|0\rangle_{\mathrm{a}M} \rightarrow \alpha_0|0\rangle|0\rangle_{\mathrm{a}1}|0\rangle_{\mathrm{a}2}\cdots|0\rangle_{\mathrm{a}M} + \alpha_1|1\rangle|1\rangle_{\mathrm{a}1}|1\rangle_{\mathrm{a}2}\cdots|1\rangle_{\mathrm{a}M}. \quad (1)$$

Then, by measuring the input and the ancilla qubits we can reduce the measurement uncertainty in the detection process [2]. Effectively, we get $M + 1$ tries to determine which state each qubit is projected into and can use a majority vote to determine the correct readout [6].

The above protocol is applicable to any quantum system. For QIP, any of the possible physical implementations being considered [7] would benefit; here, we describe how it might be implemented with atomic qubits. To explain our particular implementation, first consider an idealized experiment, where we assume that all operations other than detection are error-free. We distinguish the two states of each atom, from now on labeled $|\downarrow\rangle$ and $|\uparrow\rangle$, by observing state-dependent laser driven fluorescence of the atom. We assume that if the atom is in the $|\uparrow\rangle$ state, laser-beam scattering is absent and that for the $|\downarrow\rangle$ state, the atom can scatter many photons. Even if we detect only a small fraction of the scattered photons, we can distinguish the two states [8]. However, here, we also assume that detected photons from background light can cause us to misidentify the $|\downarrow\rangle$ state when the atom is actually in the $|\uparrow\rangle$ state. We further assume that the duration available for detection is limited by other experimental considerations (such as optical pumping of the $|\uparrow\rangle$ to the $|\downarrow\rangle$ state, which can lead to systematic errors). This situation is depicted in Fig. 1.

For one qubit, to distinguish the two states, $|\downarrow\rangle$ and $|\uparrow\rangle$, using the number of detected photons n_{det}, one must define a threshold n_1 (which depends on the duration of the detection). If $n_{\mathrm{det}} > n_1$, the state is read out as $|\downarrow\rangle$; if $n_{\mathrm{det}} \leq n_1$, the state is read out as $|\uparrow\rangle$. If the detected counts occur in the regions where the distributions $D_\uparrow$ for $|\uparrow\rangle$ and $D_\downarrow$ for $|\downarrow\rangle$ overlap, the state assignment is ambiguous. Assuming no *a priori* knowledge of measurement outcomes, the optimum value of n_1 is determined by minimizing simultaneously the fractions of $D_\uparrow$ with $n_{\mathrm{det}} > n_1$ and $D_\downarrow$ with $n_{\mathrm{det}} \leq n_1$. The average error is determined by the normalized sum of the experiments in the $D_\uparrow$ histogram for $n_{\mathrm{det}} > n_1$ and the $D_\downarrow$ histogram for $n_{\mathrm{det}} \leq n_1$. Importantly, the overlap, and therefore the average error, is much smaller for two qubits in the same state $|\downarrow\rangle|\downarrow\rangle$ with distribution $D_{\downarrow\downarrow}$ or $|\uparrow\rangle|\uparrow\rangle$ with distribution $D_{\uparrow\uparrow}$ $(= D_\uparrow)$ and the decision threshold n_2 being determined in the same manner as that for n_1. We can therefore increase our detection efficiency if we first carry out the encoding $(\alpha_\downarrow|\downarrow\rangle + \alpha_\uparrow|\uparrow\rangle)|\downarrow\rangle_a \rightarrow \alpha_\downarrow|\downarrow\rangle|\downarrow\rangle_a + \alpha_\uparrow|\uparrow\rangle|\uparrow\rangle_a$ and measure the fluorescence from both qubits [9]. As indicated in Fig. 2, the histogram overlaps and corresponding detection errors decrease as the detection duration increases.

In our experimental realization, the qubits' logical states are given by the two hyperfine states of $^9Be^+$ atomic ions $|\downarrow\rangle \equiv |F = 2, m_F = -2\rangle$ and $|\uparrow\rangle \equiv |F = 1, m_F = -1\rangle$ of the $^2S_{1/2}$ electronic ground state, separated by the hyperfine splitting $\omega_0 \simeq 2\pi \times 1.25$ GHz [10]. The ions are confined to the axis of a linear radio-frequency trap [11]. Single-qubit rotations (single bit gates) are accomplished by driving two-photon stimulated Raman transitions with the use of two laser beams ($\lambda \approx 313$ nm), whose wave

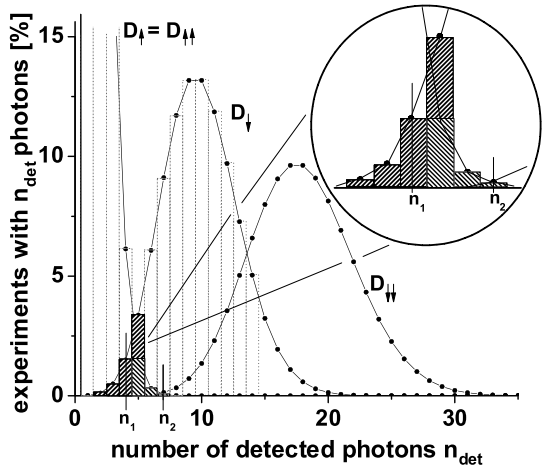

FIG. 1. Simulated Poissonian distributions D of photon counts for the detection of fluorescence in the case of (left to right) zero, one, or two qubits in the $|\downarrow\rangle$ state (the state that scatters photons). Background noise counts are responsible for the finite photon counts in $D_\uparrow$. For the plot shown, the rate of background noise counts $\langle \dot{n}_{\mathrm{bkg}} \rangle = 0.125 \langle \dot{n}_\downarrow \rangle$, where $\langle \dot{n}_\downarrow \rangle = \frac{1}{2}\langle \dot{n}_{\downarrow\downarrow} \rangle = 2.5 \times 10^4\ \mathrm{s}^{-1}$ is the count rate for the $|\downarrow\rangle$ state and where the detection duration is taken to be 324 μs (the parameters are chosen to correspond to the actual experiment). The state determination is ambiguous for detected counts n_{det} in the region where the $D_\uparrow$ and the $D_\downarrow$ distributions overlap (see magnified inset), leading to errors. In the case of one- qubit, a threshold n_1 must be determined to distinguish the two states. For two qubits being either in the $|\downarrow\rangle|\downarrow\rangle$ state with distribution $D_{\downarrow\downarrow}$ or in the $|\uparrow\rangle|\uparrow\rangle$ state with distribution $D_{\uparrow\uparrow}$, the corresponding threshold n_2 always provides a smaller overlap of the distributions, thus a smaller readout error.

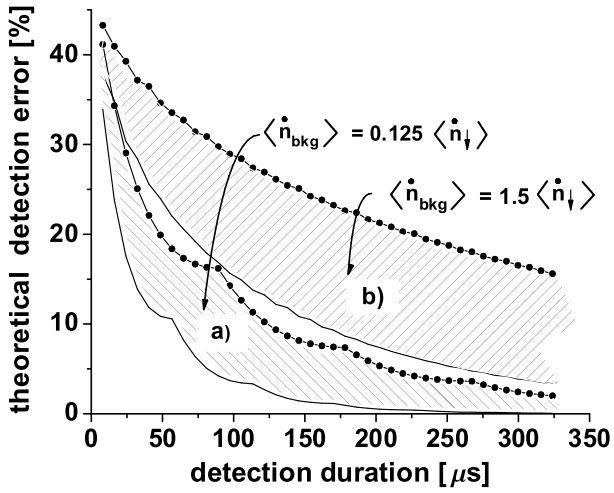

FIG. 2. Theoretical error in state identification as a function of the detection duration at a given average count rate $\langle \dot{n}_\downarrow \rangle = 2.5 \times 10^4\ \mathrm{s}^{-1}$, for two levels of background noise. The one-qubit cases (without encoding) are represented by the dotted lines, and the one-ancilla encoded case by the solid lines. The shaded areas emphasize the reduction of the error by the encoded detection scheme. We assume a background count rate of $\langle \dot{n}_{\mathrm{bkg}} \rangle = 0.125 \langle \dot{n}_\downarrow \rangle$ in the lower pair of curves (a) and of $\langle \dot{n}_{\mathrm{bkg}} \rangle = 1.5 \langle \dot{n}_\downarrow \rangle$ in the upper pair of curves (b). Since the photon number thresholds (see Fig. 1) are integers, the curves can show steps where n_1 and n_2 change.

vector difference $\Delta\vec{k} = \vec{k}_2 - \vec{k}_1$ is aligned along the trap axis ($|\Delta k| = \sqrt{2} \times 2\pi/\lambda = 2\pi/\lambda_{\text{eff}}$) and whose frequency difference $\omega_2 - \omega_1$ is equal to ω_0. Such a rotation on a state vector can be represented by

$$\begin{pmatrix} \alpha'_\downarrow \\ \alpha'_\uparrow \end{pmatrix} = R(\Theta, \Phi)\begin{pmatrix} \alpha_\downarrow \\ \alpha_\uparrow \end{pmatrix} = \begin{pmatrix} \cos\left(\frac{\Theta}{2}\right) & ie^{i\Phi}\sin\left(\frac{\Theta}{2}\right) \\ ie^{-i\Phi}\sin\left(\frac{\Theta}{2}\right) & \cos\left(\frac{\Theta}{2}\right) \end{pmatrix}\begin{pmatrix} \alpha_\downarrow \\ \alpha_\uparrow \end{pmatrix}. \quad (2)$$

This single-qubit gate can be visualized on the Bloch sphere [12]. The angle Θ is proportional to the duration of the Raman beam pulse, and Φ is a phase factor that depends on the phase difference of the Raman beams at the position of the ion, defining the axis about which the Bloch vector rotates. In our experiment, the conditional logic is implemented with a two-qubit geometrical-phase gate [13]. For the logical states of two qubits, the gate implements the following transformation:

$$\begin{aligned} |\downarrow\rangle|\downarrow\rangle &\rightarrow |\downarrow\rangle|\downarrow\rangle; \qquad |\uparrow\rangle|\uparrow\rangle \rightarrow |\uparrow\rangle|\uparrow\rangle, \\ |\downarrow\rangle|\uparrow\rangle &\rightarrow e^{i(\pi/2)}|\downarrow\rangle|\uparrow\rangle; \qquad |\uparrow\rangle|\downarrow\rangle \rightarrow e^{i(\pi/2)}|\uparrow\rangle|\downarrow\rangle. \end{aligned} \quad (3)$$

We denote this gate by G. For experimental convenience, we initialize the ancilla in a superposition state by a technique described below, so that the initial state of the two qubits is

$$\Psi_{\text{initial}} = (\alpha_\downarrow|\downarrow\rangle + \alpha_\uparrow|\uparrow\rangle)(|\downarrow\rangle_a + |\uparrow\rangle_a), \quad (4)$$

where not all states are normalized to simplify the expression. We now implement the operation

$$\Psi_{\text{initial}} \rightarrow R_a\left(\frac{\pi}{2}, \pi\right)G\Psi_{\text{initial}} = \alpha_\downarrow|\downarrow\rangle|\downarrow\rangle_a + \alpha_\uparrow|\uparrow\rangle|\uparrow\rangle_a, \quad (5)$$

where the R_a denotes a rotation that applies only to the ancilla. The experiment consists of applying the transformation in Eq. (5) followed by measurement of the state-dependent photon scattering from both qubits. We examine three input cases: (i) $\alpha_\downarrow = 1$, (ii) $\alpha_\uparrow = 1$, and (iii) $\alpha_\downarrow = \alpha_\uparrow = \frac{1}{\sqrt{2}}$.

At the start of each experiment, the motion of the qubits along the trap axis is cooled to the ground state, and the ions are initialized in the $|\downarrow\rangle|\downarrow\rangle_a$ state via optical pumping [14]. State preparation [Eq. (4)] and the encoding [Eq. (5)] require individual addressing of the qubits. This can be accomplished with laser-beam focusing on sufficiently separated ions [15] but can also be realized with tightly confined ions [16] and laser beams having spot sizes much larger than the spacing of the ions [17–19]. In this technique, rotations are broken into two segments in which Φ on one of the ions is switched by π between the segments by appropriately shifting the position of that ion in the laser beams.

For case (i) the phase gate transforms the state $|S_1\rangle = |\downarrow\rangle(|\downarrow\rangle_a + |\uparrow\rangle_a) = |\downarrow\rangle|\downarrow\rangle_a + |\downarrow\rangle|\uparrow\rangle_a \rightarrow |\downarrow\rangle|\downarrow\rangle_a + e^{i(\pi/2)}|\downarrow\rangle|\uparrow\rangle_a = |\downarrow\rangle(|\downarrow\rangle_a + e^{i(\pi/2)}|\uparrow\rangle_a)$ and, analogously for case (ii), $|S_2\rangle \rightarrow |\uparrow\rangle(e^{i(\pi/2)}|\downarrow\rangle_a + |\uparrow\rangle_a)$. While the primary qubit remains unchanged, the ancilla is in a superposition state with a phase dependent on the primary qubit's initial state. This phase information is converted into opposite ancilla states in the measurement basis by a second individual addressing rotation [17–19]. This last operation is identical for all three cases and composed of a $R(\frac{\pi}{4}, \pi) \otimes R_a(\frac{\pi}{4}, \pi)$ pulse followed by a $R(\frac{\pi}{4}, 0) \otimes R_a(\frac{\pi}{4}, \pi)$ pulse. For all three cases, and in general for arbitrary $\alpha_{\downarrow,\uparrow}$, this procedure implements the operation in Eq. (5). After these pulse sequences, state-sensitive detection is realized with an additional laser beam, tuned to a cycling transition [10]. The number of detected photons n_{det} is measured in a time-resolved way; that is, the counts are binned into time intervals of 10 μs (8.1 μs detection duration plus 1.9 μs dead time), providing a maximal detection duration of 324 μs (400 μs including the dead time). Data from 10^4 such experiments are used here. For our experimental optical collection and detection efficiency, a single ion in the state $|\downarrow\rangle$ provides a count rate $\langle\dot{n}_\downarrow\rangle = \frac{1}{2}\langle\dot{n}_{\downarrow\downarrow}\rangle = 2.5 \times 10^4\ \text{s}^{-1}$. In the experiment, we have $\langle\dot{n}_{\text{bkg}}\rangle \ll \langle\dot{n}_\downarrow\rangle$ and the detection efficiency is quite high. Therefore, to investigate the fundamental features of the enhancement scheme, we add Poissonian count noise to the detected ion fluorescence [20]. For the data presented here, we include two background noise levels with mean count rates $\langle\dot{n}_{\text{bkg}}\rangle = 0.125\langle\dot{n}_\downarrow\rangle$ and $1.50\langle\dot{n}_\downarrow\rangle$. To compare the two-qubit detection results with those of the one-qubit case, we perform a separate experiment with only one qubit and determine the average detection error as described in Fig. 1. The results of cases (i) and (ii) combined are shown in Fig. 3.

Even though the qualitative behavior of the protocol is verified, the experimental performance is degraded as seen by comparing Figs. 2 and 3. In Fig. 2, perfect gate operations were assumed. In the experiment, the fidelity for each two-qubit individual addressing gate (applied twice) is about 0.95 whereas rotations applied to a single ion have a fidelity greater than 0.99. The conditional phase gate has a fidelity of about 0.97 and $|\uparrow\rangle \rightarrow |\downarrow\rangle$ optical pumping causes an error smaller than 1% for our detection durations. These errors have both correlated and uncorrelated components. The net effect is that, for example, when encoding the $|\uparrow\rangle$ input state, ideally we expect probabilities $P_{\uparrow\uparrow} = 1$ and $P_{\downarrow\uparrow} + P_{\uparrow\downarrow} + P_{\downarrow\downarrow} = 0$, whereas the experiment gave $P_{\downarrow\uparrow} + P_{\uparrow\downarrow} \simeq 0.085$ and $P_{\downarrow\downarrow} \simeq 0.02$. Similar imperfections were obtained for encoding the $|\downarrow\rangle$ state. Simulations of the experiments with these distributions agree with the data (solid lines in Fig. 3) to within 1%. The higher the noise level, the more advantageous the encoding scheme, as is indicated for the case where $\langle\dot{n}_{\text{bkg}}\rangle = 1.5\langle\dot{n}_\downarrow\rangle$.

Case (iii) tests the universality of the encoding scheme for superposition states, as described by Eq. (1). The observed count histograms were an equal mixture of histo-

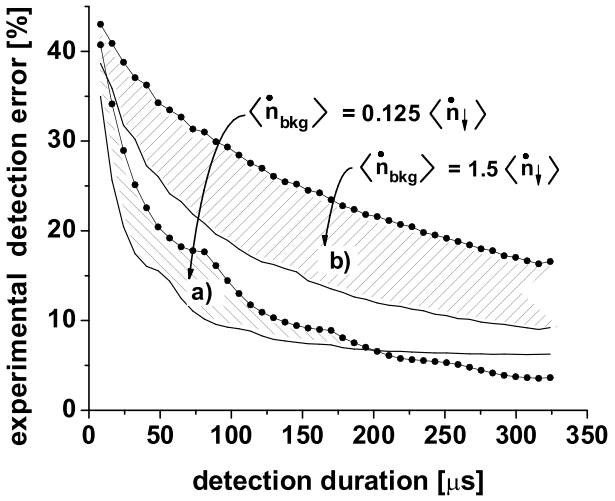

FIG. 3. Experimental error in state identification as a function of the duration of the detection at a given average count rate $\langle \dot{n}_{\downarrow} \rangle = 2.5 \times 10^4\ \mathrm{s}^{-1}$. As for the simulated results shown in Fig. 2, we examine two cases, with (a) $\langle \dot{n}_{\mathrm{bkg}} \rangle = 0.125 \langle \dot{n}_{\downarrow} \rangle$ and (b) $\langle \dot{n}_{\mathrm{bkg}} \rangle = 1.5 \langle \dot{n}_{\downarrow} \rangle$. The differences between Figs. 2 and 3, notably the leveling off of the error probability for long detection times in the encoding cases, are primarily due to the infidelity in the experimental gates required for state preparation and implementing the enhancement protocol (see the text).

grams for the $|\downarrow\rangle$ and $|\uparrow\rangle$ cases, so we used the photon thresholds n_2 determined from the results of cases (i) and (ii). With the encoding protocol, the derived coefficients of the initial superposition state are in agreement with the ideally expected ones, but in this case, noise is dominated by projection noise.

The fidelities achieved in the current experiment are not high enough for scalable QIP; however, if they can be made sufficiently high, a method like the one described here is advantageous, with significant improvements in efficiency as more ancilla qubits are used. For example, if a majority vote is used for the state of Eq. (1) (assuming an even number M of ancilla qubits) and we have a readout fidelity F, the probability to get m correct answers is $P_m = F^m(1-F)^{M+1-m}(M+1)!/[m!(M+1-m)!]$ (the binomial distribution). The probability of a correct majority vote is then $P = \sum_{m=M/2+1}^{M+1} P_m$. For example with $F = 0.7$ one needs 30 ancilla qubits to get $P > 0.99$; with $F = 0.9$ only four ancilla qubits are required.

A slight modification of the protocol presented here is to simply discard experiments when the number of detected counts is in the ambiguous region where the distributions overlap. The use of ancilla qubits shrinks the region of overlap and therefore reduces the number of experiments to be discarded. This strategy may be useful in encoded-qubit error correction or to purify special states such as Bell states [21]. Another detection strategy would be to map the state of the initial qubit onto another qubit that is more easily detected [22].

The work described was supported by ARDA/NSA and NIST. T. S. acknowledges a Deutsche Forschungsgemeinschaft research grant. We thank J. Bollinger and W. Oskay for helpful comments on the manuscript.

*Electronic address: tschaetz@mpq.mpg.de
†Present address: Department of Physics, University of Otago, Dunedin, NZ.

[1] M. A. Nielsen and I. L. Chuang, *Quantum Computation and Quantum Information* (Cambridge University Press, Cambridge, 2000), 1st ed.
[2] D. P. DiVincenzo, *Scalable Quantum Computers*, edited by S. L. Braunstein, H.-K. Lo, and P. Kok Wiley-VCH, Berlin, 2001).
[3] W. M. Itano *et al.*, Phys. Rev. A **47**, 3554 (1993).
[4] P. W. Shor, in *Proceedings of the 35th Annual Symposium on the Foundations of Computer Science*, edited by S. Goldwasser (IEEE Computer Society, Los Alamitos, CA, 1994), Vol. 35, p. 124.
[5] W. K. Wootters and W. H. Zurek, Nature (London) **299**, 802 (1982).
[6] The measurement can be made nearly as accurately as the quantum gates by applying controlled-nots in a tree-like fashion from each ancilla already prepared to two new ancillae. Note that entanglement is generated in the mapping of Eq. (1) but is not a requirement, since mapping to a mixed state gives the same advantage; e.g., for two qubits $\rho_0 \equiv (\alpha_0|0\rangle + \alpha_1|1\rangle)(\alpha_0^*\langle 0| + \alpha_1^*\langle 1|) \otimes |0\rangle\langle 0|_{a1} \rightarrow |\alpha_0|^2|0\rangle\langle 0| \otimes |0\rangle\langle 0|_{a1} + |\alpha_1|^2|1\rangle\langle 1| \otimes |1\rangle\langle 1|_{a1}$.
[7] See, for example, http://qist.lanl.gov/
[8] R. Blatt and P. Zoller, Eur. J. Phys. **9**, 250 (1988).
[9] We could also detect the qubits *separately*. In the case of one ancilla, the total error is not reduced, but if the separate answers disagree, it can be considered as a detected error. If the part of the computation leading to this detected error can be discarded and recomputed until the answers agree, then the net error is reduced [2].
[10] C. Monroe *et al.*, Phys. Rev. Lett. **75**, 4714 (1995).
[11] M. A. Rowe *et al.*, Quantum Inf. Comput. **2**, 257 (2002).
[12] L. Allen and J. H. Eberly, *Optical Resonance and Two-Level Atoms* (Dover, New York, 1987).
[13] D. Leibfried *et al.*, Nature (London) **422**, 412 (2003).
[14] B. E. King *et al.*, Phys. Rev. Lett. **81**, 1525 (1998).
[15] H. C. Nägerl *et al.*, Phys. Rev. A **60**, 145 (1999).
[16] Small ion separations are desirable because logic-gate durations are reduced as the confinement strength increases.
[17] D. Kielpinski *et al.*, Science **291**, 1013 (2001).
[18] M. A. Rowe *et al.*, Nature (London) **409**, 791 (2001).
[19] T. Schaetz *et al.*, Phys. Rev. Lett. **93**, 040505 (2004).
[20] The background noise can be added by adjusting the level of detected stray scattered light, but we found it more convenient for the purpose of our demonstration to add it numerically.
[21] C. H. Bennett *et al.*, Phys. Rev. Lett. **76**, 722 (1996); **78**, 2031(E) (1997).
[22] D. J. Wineland *et al.*, in *Proceedings of the 6th Symposium Frequency Standards and Metrology*, edited by P. Gill (World Scientific, Singapore, 2002), pp. 361–368.